

RESEARCH NOTE

A pilot study on the measurement of central posterior corneal radius in Hong Kong Chinese using Purkinje image technique

Andrew K. C. Lam¹ and William A. Douthwaite²

¹Department of Optometry and Radiography, Hong Kong Polytechnic University, Hong Kong; and ²Department of Optometry, University of Bradford, Bradford, UK

Summary

The central posterior corneal radius was measured by assessing the first and second Purkinje images produced from a modified keratometer. This method was initially assessed by measuring five PMMA lens buttons with back surface radii from 6.2 mm to 7.0 mm. It was reasonably accurate when compared with the measurements made using a conventional radiuscope. The technique was found to be repeatable for human subjects measured on three separate occasions. The mean central posterior corneal radii from a group of 30 Hong Kong Chinese were 6.64 mm (SE 0.05 mm) and 6.39 mm (SE 0.05 mm) along the horizontal and vertical meridians respectively. These results are similar to previous studies using a similar technique. The posterior corneal radii were found to be similar for right and left eyes and there were no gender differences. Copyright © 1996 The College of Optometrists. Published by Elsevier Science Ltd.

Introduction

The posterior corneal curvature has been difficult to assess using Purkinje image methods because the second Purkinje image is so dim. An early method of studying the posterior corneal curvatures was introduced by Lowe and Clark (1973), who used corneal section photography. A photograph of the corneal section in the vertical meridian was matched with curves containing different radii. With the knowledge of the anterior corneal curvature, the true posterior corneal radius of curvature can be found by ray tracing. The main drawback of this method arises from the assumption of a spherical surface for both the anterior and the posterior cornea.

A more recent method utilising Purkinje image photography has been used in the study of posterior corneal surface toricity (Royston *et al.*, 1990a; Dunne *et al.*, 1992). A Canon autorefractor R-1 was used with the original infrared light sources replaced by four extra light sources along three different meridians, horizontal, 45° and vertical. This principle used a Purkinje image ratio (p) which is

defined as the size of the second Purkinje image divided by the size of the first Purkinje image (Royston *et al.*, 1990b).

Purkinje image ratio $p =$

$$\frac{\text{second corneal Purkinje image height}}{\text{first corneal Purkinje image height}} = \frac{r'_2}{r_1} \quad (1)$$

where r'_2 is the apparent posterior corneal radius from the apparent position of the posterior corneal surface, and r_1 is the radius of curvature of the anterior cornea.

Since the first Purkinje image size is directly proportional to the anterior corneal radius for collimated mires, the second Purkinje image size is related to the apparent posterior corneal radius.

Figure 1 illustrates that if the posterior cornea is considered as an object, the apparent position of the posterior corneal surface after refraction by the anterior cornea can be calculated from

$$d' = \frac{1}{\frac{n}{d} - F_1} \quad (2)$$

where d (in metres) is the true corneal thickness, d' (in metres) is the apparent corneal thickness, F_1 is the

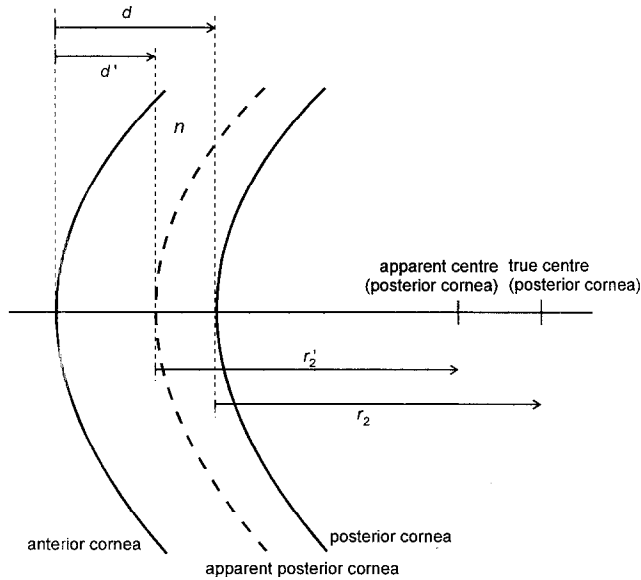


Figure 1. Location of the apparent posterior cornea.

refractive power of the anterior corneal surface, and n is the corneal refractive index.

After refraction by the anterior cornea, not only is the location of the posterior cornea changed, but the image of the centre of curvature is also altered. When the distance from the true centre of curvature of the posterior cornea to the anterior cornea ($r_2 + d$) is considered as an object, the apparent position of the centre of curvature of the posterior cornea ($r'_2 + d'$) after refraction by the anterior cornea can be calculated. The true posterior corneal radius r_2 is,

$$r_2 = \frac{n}{F_1 + \frac{1}{r'_2 + d'}} - d \quad (3)$$

The modification in the study of Royston *et al.* (1990b) is simple but the Canon autorefractor R-1 is no longer available in the market. Thus, a similar modification was made to another instrument for posterior corneal surface measurement. Its accuracy was assessed using PMMA lens buttons and the instrument was applied *in vivo* measurements in Chinese eyes.

Modification of the instrument

A Sun SK-2000 (Sun Contact Lens, Japan) topographic keratometer was modified. This topographic keratometer measures the central cornea at 2.5 mm diameter and peripherally at 8 mm diameter (Dave *et al.*, 1995). The modification involved installation of four extra LEDs with two LEDs placed along the horizontal and two along the vertical meridians. A black plastic circular plate was used to hold the LEDs in place. Each LED was placed 50 mm from the centre of the plate to ensure adequate separation of the 1st

and 2nd Purkinje images. A central circular aperture of 11 mm diameter was cut on the plate to allow the camera inside the keratometer to capture the reflected images of the extra LEDs. Since the keratometer has two built-in LEDs aligned in the vertical meridian, the small aperture also helps to prevent any reflection from the existing LEDs on the cornea. The reflection was found to be maximum when the extra LEDs were placed with their emission axes making an angle of about 50° to the optical axis of the instrument (Figure 2). These LEDs were supplied by a 9 V direct current source. A Mitsubishi video printer (Mitsubishi Electric Corporation, Japan) was connected to the keratometer to print out the Purkinje images.

Measurement of lens buttons

Five lens buttons made of PMMA ($n = 1.49$) were ordered from a local contact lens laboratory. The front and back surfaces of these lenses were monocurve with an overall lens diameter of 10 mm. The back surface radii of these lenses ranged from 6.2 mm to 7.0 mm, which covers the normal range of the human central posterior corneal radius (Dunne *et al.*, 1991). The back surface radius of each lens was determined by a Shin-Nippon radiuscope (Mitutoyo Corporation, Japan) with a precision of 0.01 mm. Ten readings were taken and averaged for each lens button. The back surface radius of each lens button was then assessed using the Purkinje image technique as follows.

Firstly, the front surface radius of each lens was measured by a conventional Bausch and Lomb keratometer. This keratometer was calibrated using steel balls of radii from 6.5 mm to 9.0 mm. The centre thickness of each lens was measured using the digital thickness gauge of the Shin-Nippon radiuscope (Mitutoyo Corporation, Japan). The front surface radius and lens thickness were both measured

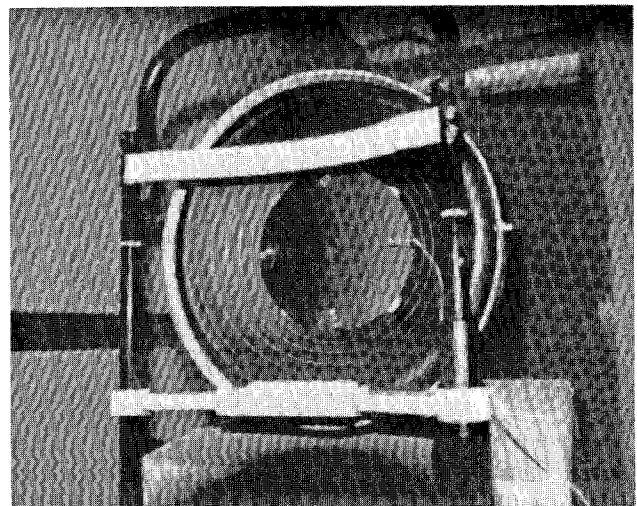


Figure 2. Photograph showing the modification of topographic keratometer.

ten times and the averaged values were used for analysis. The reflected images of the LEDs from the front and back surfaces of each lens were printed by the video printer (Figure 3). The sizes of images (centre to centre distance) reflected from the front surface (AB) and back surface (ab) were measured with a vernier calliper with 0.02 mm divisions. The back surface radius was calculated from the measured images using equation (3) where:

n is the refractive index of PMMA, 1.49,

d is the lens thickness determined by the digital thickness gauge,

r'_2 is derived from the Purkinje image ratio (p) and the front surface radius using equation (1)

F_1 is the front surface power of the lens determined by keratometry

d' is calculated from n , d , and F_1 using equation (2)

The 'calculated' back surface radius was compared with the back surface radius determined using the radiuscope.

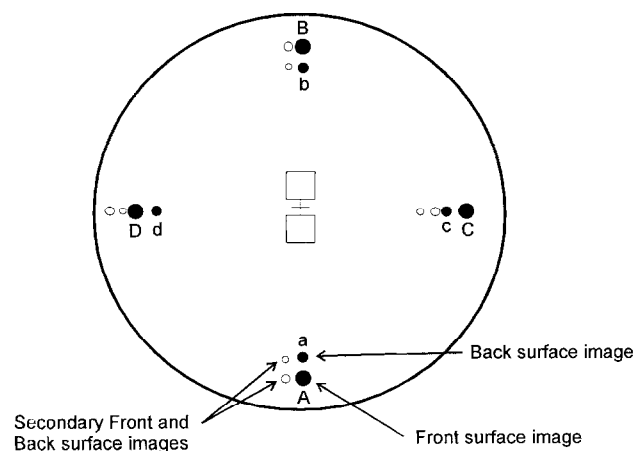
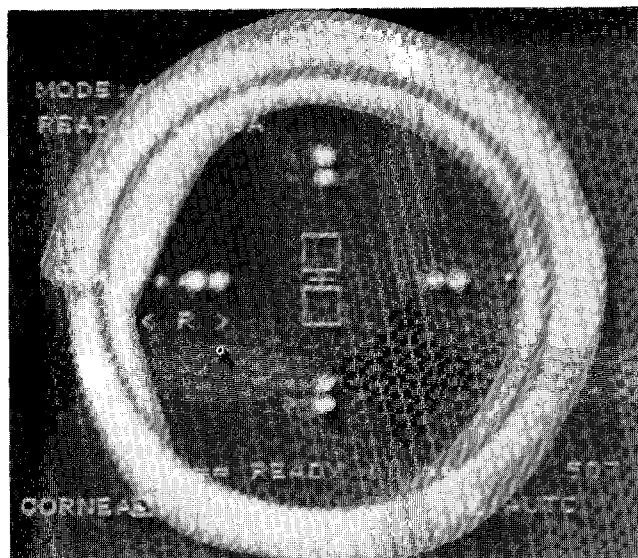


Figure 3. Photograph of the reflected images on lens buttons.

Accuracy

The back surface radii determined using the radiuscope, the Purkinje image methods and their differences are given in Table 1.

A significant correlation was found between the back surface radii obtained from these two methods (Figure 4: $r = 0.999$, $P < 0.001$, $y = 1.03x - 0.18$). However, the use of 95% limits of agreement (mean difference $\pm 1.96 \times$ standard deviation of the differences) can better assess the agreement of two different methods (Bland and Altman, 1986; Zadnik *et al.*, 1992). The mean difference between these two methods was 0.018 mm (SD 0.016 mm). This mean difference (bias) was not significantly different from zero (one sample t-test: $t = 2.469$, $P = 0.069$). The 95% limits of agreement were ± 0.03 mm. The posterior corneal radius determined from the Purkinje image technique in the following study was treated as the true value.

Table 1. Back surface radii of lens buttons determined using Purkinje image method (A) and Radiuscope (B)

	Back surface radius measured by		
	Purkinje image method (A)	Radiuscope (B)	Difference (B - A)
Lens A	6.994 mm	7.029 mm	0.035 mm
Lens B	6.795 mm	6.815 mm	0.020 mm
Lens C	6.598 mm	6.624 mm	0.026 mm
Lens D	6.439 mm	6.430 mm	-0.009 mm
Lens E	6.206 mm	6.225 mm	0.019 mm

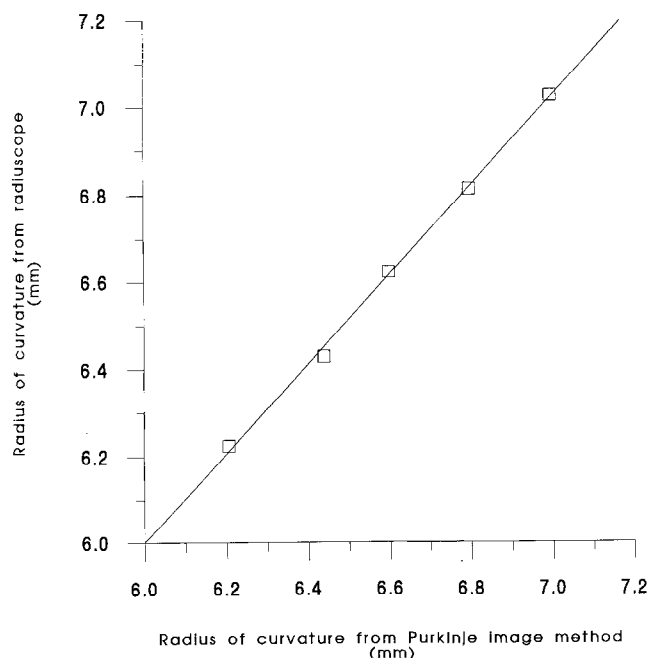


Figure 4. Regression line showing the relationship between the results from the radiuscope and the Purkinje image methods: ($y = 1.03x - 0.18$, $R = 0.999$, $P < 0.001$)

Measurement of the human cornea

This Purkinje image technique was used to measure the *in vivo* central posterior cornea on human subjects. The repeatability of the method was first assessed by measuring the cornea of ten subjects at approximately the same time of day on three different days. All the subjects had healthy corneas by slit-lamp examination and only the right eye was examined. The same procedures, including the measurement of the anterior corneal radius, measurement of corneal thickness, and Purkinje image photography, were carried out at each trial.

The anterior central corneal radius was measured using a Bausch and Lomb keratometer. The subject was instructed to fixate the image of his/her own eye produced by reflection from a mirror incorporated in the instrument. An Alcon ultrasound pachometer (Alcon Laboratories Inc., Texas, USA) was used to measure the central corneal thickness of each subject. This pachometer has a measurement range from 200 to 1300 μm with a resolution of 1 μm . The transducer frequency is 20 MHz and the probe diameter 1.5 mm. The pachometer was calibrated using a 'Calibration Box' provided by the manufacturer. When this system is attached to the main unit, it emits an ultrasound signal and if the pachometer gives a reading of $800 \pm 5 \mu\text{m}$, it is considered to be accurate enough to interpret the real echoes from the ultrasound probe. The accuracy of this instrument is claimed to be $\pm 5 \mu\text{m}$. A Probe Quality Test was performed automatically after switching the power on each time to test the function of the probe. Pilot testing established that ten readings were sufficient to provide an accurate assessment of corneal thickness; mean values were then calculated for 10 repeat readings on each subject.

When measuring lens button thickness, a digital thickness gauge was used instead of an ultrasound pachometer, as used in measuring human corneal thickness, because the latter did not yield reliable results. This may have been due to the difference in ultrasound velocity in the lens material compared with its calibrated velocity for the human cornea. The instrument was then calibrated using the calibration box provided by the manufacturer only. The repeatability of the corneal thickness measurement can be improved by measuring the cornea at exactly the same location each time. This was achieved in the current study by putting the transducer probe on a microscope-type X-Y plate to control the lateral and antero-posterior movement of the probe. The subject used a chin-rest to further reduce any relative movement between the eye and probe.

For Purkinje image photography, the subject was instructed to fixate the flashing target inside the topographic keratometer. Purkinje images were recorded using the modified topographic keratometer and video printer. From Figure 5, the first and second Purkinje image sizes along the horizontal meridian are CD and cd respectively. The first and second Purkinje image sizes along the vertical meridian are AB and

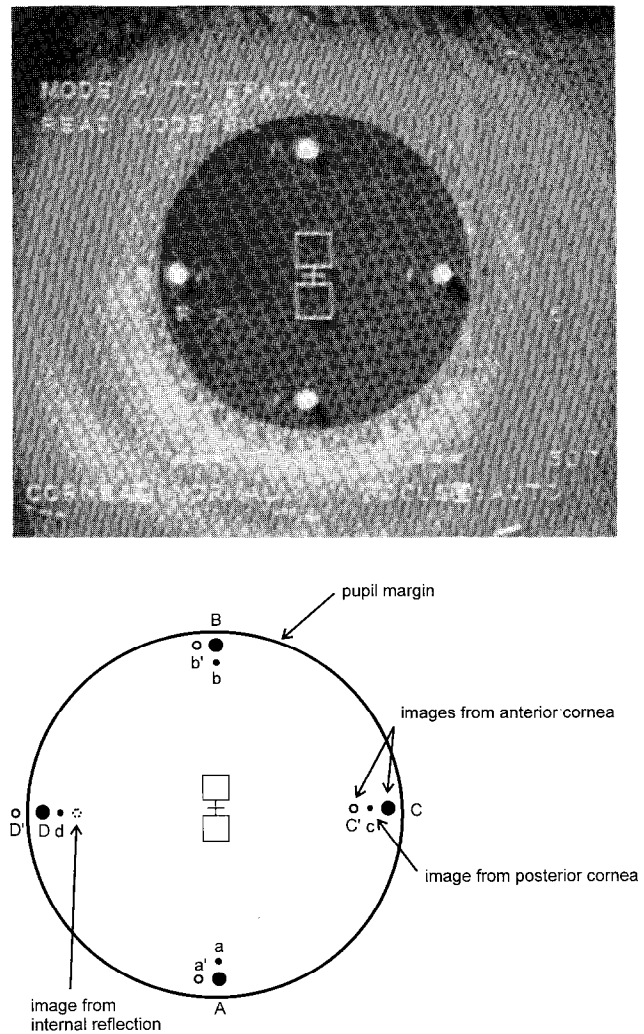


Figure 5. Photograph of the reflected images on human cornea.

ab respectively. Three images were recorded and the mean Purkinje image ratio was used for analysis. Equation (3), was used to calculate the posterior corneal radius. The refractive index of the cornea (n) was assumed to be 1.376 as in Gullstrand's Exact Schematic Eye (Tunnacliffe, 1993).

The sizes of the reflected images from the lens buttons and also the Purkinje images of the human cornea were measured with a vernier calliper. This method was similar to that used by van Veen and Goss (1988). Measurements were repeated five times on each photograph and the mean values used for analysis.

After the repeatability test on ten subjects, further measurements were made on 30 University students. Right and left eyes were assessed. All had healthy corneas revealed by slit-lamp examination.

Results

Five parameters were assessed in the repeatability study;

these were the Purkinje ratios along the horizontal and vertical meridians, the central corneal thickness, and the corneal radii calculated for the horizontal and vertical meridians. A Repeated Measures ANOVA indicated that all five parameters were similar on different trials without any significant difference (*Table 2*).

Thirty students (12 females and 18 males) with a median age of 20 years were recruited for the main study. Their averaged central corneal thickness was 553.5 μm (SD 34.2 μm) for the right eye and 552.0 μm (SD 33.6 μm) for the left eye. The mean posterior corneal radii along the horizontal and vertical meridians were 6.63 mm (SD 0.28 mm) and 6.38 mm (SD 0.25 mm), respectively, for the right eye, and 6.65 mm (SD 0.27 mm) and 6.40 mm (SD 0.32 mm), respectively, for the left eye.

There were no significant differences between the two eyes in corneal thickness (Paired t-test: $t = 1.03$, $df = 29$, $P = 0.31$), posterior corneal radii along the horizontal (Paired t-test: $t = -1.28$, $df = 29$, $P = 0.21$) or vertical meridian (Paired t-test: $t = -0.72$, $df = 29$, $P = 0.48$). The results from the right and left eyes were therefore averaged for further statistical analysis.

The averaged anterior corneal radii along the horizontal and vertical meridians were 7.87 mm and 7.66 mm respectively (Paired t-test: $t = 9.90$, $df = 29$, $P < 0.001$). As for the anterior cornea, the averaged posterior corneal radius was flatter in the horizontal meridian, 6.64 mm, than in the vertical meridian, 6.39 mm (Paired t-test: $t = 9.27$, $df = 29$, $P < 0.001$). The anterior and posterior corneal surface radii were highly correlated along both the horizontal and vertical meridians (horizontal: $r = 0.87$, $P < 0.001$; vertical: $r = 0.90$, $P < 0.001$).

There was no difference between the mean corneal thicknesses measured for male and female subjects (Unpaired t-test: $t = 1.20$, $df = 28$, $P = 0.24$), or between the vertical posterior corneal radii (Unpaired t-test: $t = 1.61$, $df = 28$, $P = 0.12$). A marginal significant difference was demonstrated between the horizontal posterior corneal radii (Unpaired t-test: $t = 2.08$, $df = 28$, $P = 0.05$). The mean horizontal posterior corneal radius for males was 6.72 mm (SE 0.06 mm) and for females was 6.52 mm (SE 0.07 mm).

Discussion

The Purkinje image technique used in the current study applies the same principle as that described by Royston *et al.* (1990a). Although the instrument is different, the modification is still very simple. In fact, there are two infrared LEDs already in the topographic keratometer, but their separation is not large and they are not sufficiently oblique to isolate the first and second Purkinje images. The small central aperture on the plastic plate blocks the light from the existing LEDs to the cornea. In principle, any photographic keratometer or refractometer could be modified for use as a Purkinje image based instrument.

The lens button assessment with the Purkinje image method produced similar results to the radiuscope. However, the lens buttons were spherical and may not be an appropriate approximation for the posterior cornea. *Figure 3* illustrates that there are more than two reflected images from the anterior and posterior surfaces. This is due to multiple internal reflections of the light from the LED from the anterior and posterior corneal surfaces. It is important to ensure that measurements are made on the appropriate images (see *Figure 5*). There are even more internal reflected images on measuring human eyes (*Figure 5*).

Since the subject looked at a fixation point along the optical axis of both keratometers, these measurements were taken from the same point on the cornea which was neither the line of sight nor the visual axis as explained by others (Mandell, 1992; Mandell, 1994; Dave *et al.*, 1995). In order to use the same reference point on the cornea for different ocular parameters, the subject was asked to fixate along the axis of the transducer probe during the measurement of corneal thickness.

The principle of the instrument described here is the same as that described by Royston *et al.* (1990a), and in such instruments the central portion (actually central to mid-peripheral) of the cornea was investigated. Although the subjects used here were Chinese and Royston *et al.* (1990b) used Caucasian subjects, the findings are similar to those of both Royston *et al.* (1990b) and Dunne *et al.* (1991) (*Table 3*). Horizontal posterior corneal radii were flatter in males compared to females. This result may not

Table 2. Repeatability study of Purkinje image method of 10 subjects. Averaged results of each parameter on different trials and Repeated Measures ANOVA results

	Trials			ANOVA	
	1	2	3	F	P
Purkinje ratio, horizontal	0.820	0.832	0.827	14.35, 1.93	0.174
Posterior corneal radius, horizontal (mm)	6.585	6.664	6.629	27.83, 2.12	0.149
Central corneal thickness (μm)	561.19	563.79	560.68	28.04, 2.18	0.143
Purkinje ratio, vertical	0.823	0.823	0.827	10.45, 0.45	0.647
Posterior corneal radius, vertical (mm)	6.433	6.459	6.462	40.24, 0.54	0.592

Table 3. Posterior corneal radius results from different studies

Study	Sample size	Results
Current study	30 normal eyes (R + L averaged)	6.64 mm (SE 0.05 mm) horizontal 6.39 mm (SE 0.05 mm) vertical
Royston <i>et al.</i> , 1990b	15 normal eyes	6.40 mm
Dunne <i>et al.</i> , 1991	60 normal eyes	6.78 mm (SE 0.03 mm) horizontal 6.49 mm (SE 0.04 mm) vertical

be conclusive due to the limited number of subjects. Further investigation involving a large number of samples should be carried out.

Because of the arrangement of the extra LEDs in the instrument used here, only the horizontal and vertical meridians were considered. For other meridians, more LEDs could be added along different orientations.

There is a significant correlation between the anterior and posterior cornea, and the posterior cornea is similar to the anterior cornea in that it is flatter along the horizontal meridian than the vertical meridian. If the refractive index of the aqueous is assumed to be 1.336 as in the Gullstrand's Exact Schematic Eye (Tunnacliffe, 1993), the astigmatism of the posterior cornea is 0.25 D against-the-rule on average in these subjects.

The posterior cornea can also be determined using an instrument called the Anterior Eye Segment Analysis System (Nidek Co. Ltd., Japan). This has been developed mainly to assess the anterior chamber angle (Baez *et al.*, 1992). This equipment uses Scheimpflug photography of the anterior eye segment; the posterior corneal radius is calculated by placing 10 points manually along the posterior corneal surface using a computer mouse and the curve of the surface is fitted with a quadratic equation by a computer program (Shibata *et al.*, 1990). It has been used to study the anterior chamber angle before and after surgery in Caucasian patients (Morsman *et al.*, 1994). However, the high cost of this instrument reduces its clinical value in optometric practice.

The assumption of a spherical cornea still exists in this Purkinje image technique. The accuracy of this method may not be assured in the whole cornea due to the possibility of its asphericity. Conventional keratometry has made the same assumption of spherical cornea around an approximately 3 mm diameter region. Although the keratometric information has limited value in the study of corneal topography, it is still useful in the study of corneal power and the design of contact lenses. If measurement of the posterior corneal surface is used in the study of corneal optical performance (Dunne *et al.*, 1991) or the proposal for a four-surface schematic eye (Bennett & Rabbetts, 1989), the result obtained in the current method is still useful. For those who are interested in the entire corneal shape, then other methods (Camellin, 1990; Baez *et al.*, 1992) to investigate the corneal profile should be used.

In conclusion, the central posterior cornea can be determined *in vivo* from Purkinje image photography using a simple modification to clinical photographic keratoscopic instruments. The meridian being studied depends on the orientation of the added LEDs.

Acknowledgement

We would like to thank Dr. Brian Brown for his comments on the manuscript.

References

- Baez, K. A., Orengo, S., Gandham, S. and Spaeth, G. L. (1992). Intraobserver and interobserver reproducibility of the Nidek EAS 100 anterior segment analysis system. *Ophthalmic Surg.* **23**, 426–428.
- Bennett, A. G. and Rabbetts, R. B. (1989). Letter to editor. *Ophthalm. Physiol. Opt.* **9**, 228–230.
- Bland, J. M. and Altman, D. G. (1986). Statistical methods for assessing agreement between two methods of clinical measurement. *Lancet* **i**, 307–310.
- Camellin, M. (1990). Proposed formula for the dioptric power evaluation of the posterior corneal surface. *Refract. Corneal Surg.* **6**, 261–264.
- Dave, T. N., Fowler, C. W., Elawad, M. E. A. and Dunne, M. C. M. (1995). A clinical trial of the SUN SK-2000 computer-assisted videokeratoscope. *Ophthalm. Physiol. Opt.* **2**, 105–115.
- Dunne, M. C. M., Royston, J. M. and Barnes, D. A. (1991). Posterior corneal surface toricity and total corneal astigmatism. *Optom. Vis. Sci.* **68**, 708–710.
- Dunne, M. C. M., Royston, J. M. and Barnes, D. A. (1992). Normal variations of the posterior corneal surface. *Acta Ophthalmol.* **70**, 255–261.
- Lowe, R. F. and Clark, B. A. J. (1973). Posterior corneal curvature. Correlations in normal eyes and in eyes involved with primary angle-closure glaucoma. *Br. J. Ophthalmol.* **57**, 464–470.
- Mandell, R. B. (1992). The enigma of the corneal contour. *C.L.A.O.* **18**, 267–273.
- Mandell, R. B. (1994). Apparent pupil displacement in videokeratography. *C.L.A.O.* **20**, 123–127.
- Morsman, C. D., Lusky, M., Boses, M. E. and Weinreb, R. N. (1994). Anterior chamber angle configuration before and after iridotomy measured by Scheimpflug video imaging. *J. Glaucoma* **13**, 114–116.
- Royston, J. M., Dunne, M. C. M. and Barnes, D. A. (1990a). Measurement of posterior corneal surface toricity. *Optom. Vis. Sci.* **67**, 757–763.
- Royston, J. M., Dunne, M. C. M. and Barnes, D. A.

- (1990b). Measurement of the posterior corneal radius using slit lamp and Purkinje image techniques. *Ophthal. Physiol. Opt.* **10**, 385–388.
- Shibata, T., Sasaki, K., Sakamoto, Y. and Takahashi, N. (1990). Quantitative chamber angle measurement utilising image-processing techniques. *Ophthalmic Res.* **22**(SI), 81–84.
- Tunnacliffe, A. H. (1993). Optics of the Eye. In: *Introduction to Visual Optics*. 4th Ed. *Assoc. of Br. Dispensing Opticians*. Ch. 2, pp. 34.
- van Veen, H. G. and Goss, D. A. (1988). Simplified system of Purkinje image photography for phakometry. *Am. J. Optom. & Physiol. Optics* **65**, 905–908.
- Zadnik, K., Mutti, D. O. and Adams, A. J. (1992). The repeatability of measurement of the ocular components. *Invest. Ophthalmol. Vis. Sci.* **33**, 2325–2333.